Provenance Studies of Alluvial Tin Deposits in Parts of Ropp Younger Granite Complex, Northcentral Nigeria

Aliyu Ibrahim Kankara [1] **, Mohammed Ibrahim Mustapha** [2] **, Hamza Farouk** [3] **, Terlumun Adagba** [1]

[1] *Federal University Dutsinma*
P. M. B. 5001 Dutsin-ma, Katsina State, Nigeria

[2] *Ahmadu Bello University*
Zaria, 810211, Nigeria

[3] *National Space Research and Development Agency*
P. M. B. 437, Garki, Abuja, Nigeria

Abstract. The study area in this research is within the Ropp Complex, part of the Nigerian Mesozoic Younger Granite province. The study aims to interpret the depositional environment and establish the provenance of the alluvial cassiterite deposits in the study area. Boreholes/mining pits were logged for this study, and stanniferous sandstone samples were collected, which were used for textural and mineralogical studies. The mineral assemblages documented in the samples include ilmenite (3 to 27%). Cassiterite (2 to 14 %), Zircon (2 to 16%), magnetite (0 to 17%), tourmaline (5 to 11%), rutile (2 to 8%) and monazite (2 to 7%). The ZTR Index calculated from the result of heavy minerals analysis for the selected pieces is 59%. Mineralogical studies revealed that quartz is the most dominant detrital mineral averaging about 93-99%, indicating that the stanniferous sandstones are compositionally matured and have experienced a high degree of chemical weathering. The quartz grains have grain sizes ranging from coarse to very coarse. They are poorly sorted, sub-angular to sub-rounded, with low sphericity. This also indicates a closeness to the source and textural immaturity. The occurrence of relatively very few feldspar grains suggests a slow sedimentation rate, very high rate of chemical weathering and composition maturity. The bivariate plots, univariate grain size parameters and probability plots, and the absence of fossils and trace fossils suggest deposition in a fluvial environment. The results of the granulometric analysis indicate that the study area's stanniferous sandstone was deposited in a fluvial environment by a low-energy fluvial (river) depositional system and the deposition in proximal (close to the source). This study suggests that the Basement complex and Younger Granite are the sources of the stanniferous placer deposits.

Keywords: fluvial environment; heavy mineral; petrography; ropp complex; stanniferous sandstone.

INTRODUCTION

Provenance studies involve the interpretation of the lithologic source of sediments and/or sedimentary rocks [21]. It is one of the key elements of basin analysis, as it provides basic information regarding the tectonic origin of a sedimentary basin using compositional and textural properties of sediments. Information about the source of sediments may be obtained from examining the various clasts present [23, 1]. The most crucial aspect of provenance studies is identifying source rock, relief, the climate in the source area, tectonic settings, transport history and digenetic modifications. Provenance studies of sedimentary rocks, especially sandstones, have been carried out by many workers to extract information from compositional and textural features of sandstones, and a thorough review of the subject is given by [24]. Standard petrographical approaches to identifying source rocks of sandstone investigations of undulocity and polycrystallinity of quartz grains, types of feldspar present [23] and rock fragments [24]. The relief and climate of the source area can be inferred from grain roundness and the average degree of feldspar alteration [10]. Tectonic settings can be determined from the relative proportion of quartz,

feldspar and rock fragments [6]. Clues of sandstone's transport history can come from examining the roundness and sphericity of grains and textural and mineralogical maturity [24].

Alluvial tin deposits have been reported in the Younger Granites of mostly North Central Nigeria. [27, 28, 22]. Some of these Younger granite occurrences have also been reported in Northwestern Nigeria. [14]. The major sources of cassiterite in Nigeria are the placer (alluvial and eluvial) deposits from the biotite granites within the Jurassic alkaline ring complex (the Younger Granites) of the Jos Plateau. Placers are probably one of the earliest types of mineral deposits to have been utilized by man. Author [2] pointed out that the tin placer deposits were rarely treated as serious topics within classical tin geology, even though [4] estimated that 80 % of the world's tin production was derived from placer deposits. The lack of understanding of tin placers may be illustrated by examining the inferred distance of transport of cassiterite from the source rock. According to [8], the median transport distance from bedrock source for economic tin placer deposits is only 8 km. Other undiscovered bedrock mineralization sources were possibly contributing en route, and the dispersion could be even shorter.

Most of the published and unpublished literature on the occurrence of tin in the Younger granite focuses on the primary mineralization of tin; this shows that only a little knowledge is highlighted about the alluvial tin mineralization in the complex even though over 95% of the tin (cassiterite) produced in Nigeria was mined in the Younger Granite Province and were won from alluvial deposits derived from the tin-bearing granites and lodes [15, 16]. The rich and extensive placers of the Jos Plateau were mainly formed from the erosion of the basement rocks. During a period of elevated base level, streams aggraded their valleys and buried the placers beneath a blanket of clay and alluvium.

Study area

The study area is in parts of Ropp Complex, located southeast of the Jos Bukuru Complex in North Central Nigeria. The complex is known for its whitish riebeckite granites, extensive kaolin and tin mineralization, and long mining history. It was the second largest tin producer in the Nigerian Younger Granite Province [3]. The study area is situated in Barkin Ladi LGA within latitude 9030'00'' to 9015'00''N and longitude 8045'00'' to 8052'30''E of the Federal Survey Map sheet 189 Kurra NE (Figure 1).

The study covers an area of approximately 375 km². The area is accessible by tarred roads, untarred roads, footpaths and cattle tracks. The area is marked by high topography averaging about 1350 m above sea level. The complex is bounded by extensive actuate and polygonal ring dykes, which enclose basement rocks and the prominent central massif of rugged younger granite hills.
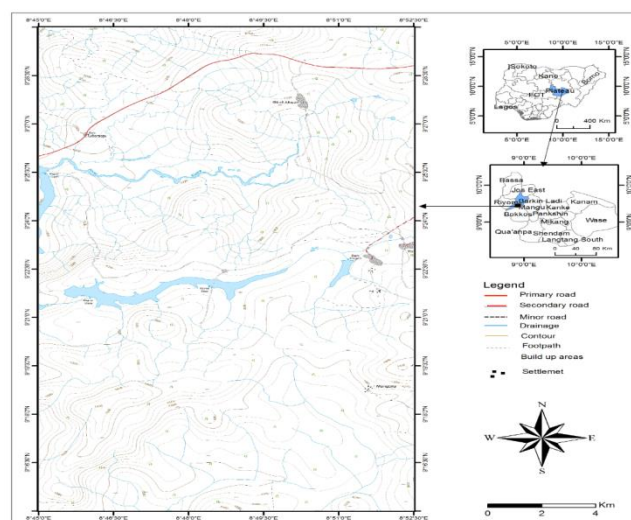

Figure 1 – Location map of the study

The drainage pattern of the area is radial and essentially controlled by the distribution of younger granite outcrops. The central river system in the study area is the River Kurra and its tributaries, draining into Monguna and Tente provinces, where dams are constructed.

MATERIALS AND METHODS

The methods employed in this research work were fieldwork and laboratory analyses. The fieldwork involved description, logging, measurement and sample collection of various lithologic units. Samples were collected for laboratory analyses. The laboratory work involves textural, petrographic and heavy minerals analyses of cassiterite-bearing sandstone samples.

Granulometric analysis. This analysis was used to determine and evaluate the grain size distribution and texture of selected samples of the stanniferous sandstones of the study area. Friable

and unconsolidated arenaceous models were the only ones subjected to sieve analysis. The samples were first disintegrated into individual grains using the ceramic mortar and pestle. Each sample was soaked with hydrogen peroxide for about 2-3 hours in a beaker. This is done to aid the disintegration of the samples further to eliminate the effect of cementation.

Each sample was placed in a sieve shaker and sieved for about 10 minutes using standard sieve openings of 2, 1, 0.6, 0.5, 0.3, 0.25, 0.15, and 0.075 mm and pan. The percentage mass retained and cumulative percentage of the group retained for each sample were determined. The methods then computed the statistical parameters (mean, standard deviation, skewness, and kurtosis) of the grain size frequency distribution [12, 18]. A probability scale was used in plotting the standard cumulative curves of grain size distribution following the procedures of [7, 26].

Petrography. Thin-section petrography of the stanniferous sandstones was carried out at the geological laboratories of Ahmadu Bello University Zaria on the ten representative samples for microscopic examination of their mineralogical composition. The samples were impregnated in epoxy before cutting and mounted on glass slides using Canada balsam. The rock slice was glued to a glass slide and was ground to 30 microns thick.

The prepared slides were then labelled and examined with the aid of transmitted light under the flat stage of the petrographic microscope. The studied thin sections were described in terms of grain contacts, roundness, grain size and sorting.

Point counting. Modal analyses of the samples were carried out using Jmicrovision v1.27 Image Analyzer. In each thin section, 300 points were counted to calculate the composition. The objective of point-counting is to identify grain types (framework), cement, matrix and their proportion for each thin section. Classification of the sandstone was determined using [10, 23] methods. Major detrital framework components of the sandstone quartz, feldspar and lithic fragments were used to construct a QFL ternary diagram.

Heavy mineral analysis

The heavy mineral analysis was carried out in the Sedimentology Laboratory of the Department of Geology, Ahmadu Bello University Zaria. The sandstones were sieved to obtain the very fine to fine sand fractions (4 phi), which are commonly analyzed because it is the size fraction likely to contain the highest percentage of heavy minerals. Two grams from each sample were weighed and poured into the centrifuge tubes containing 10 ml of the heavy liquid (bromoform). The centrifuge tubes were inserted in their respective holes in the centrifuge, and the cover was closed before running the machine for 10 minutes. Acetone was used to clean and deodorize the bromoform in the heavy minerals.

Furthermore, Magnetic separations were carried out to identify opaque heavy minerals. Although the Frantz electromagnetic separator may be used to separate minerals, it is slow. The sample can be contaminated by impurities such as rust and leftover minerals from the previous separation. So, a hand-magnet was used, which was invaluable in telling the difference between magnetite, ilmenite, and other opaque minerals.

Furthermore, the heavy minerals were identified and examined with a binocular microscope. The percentage of heavy minerals in each sample was determined using the Fleet method by counting all the grains in the mount (manually) [9]. Whenever possible, at least 200 heavy minerals were identified and counted from each slide, which is a sufficient number for characterizing the abundances of common species. The "ZTR" index was calculated using the percentage of the combined Zircon, Tourmaline and Rutile grains for each sample according to the formula below.

$$ZTR\ Index = \frac{Zircon + Tourmaline + Rutile}{Total\ No\ of\ Opaque\ Heavy\ Minerals}$$

The calculated index is expressed in percentage to ascertain the mineralogical maturity of the sediment. ZTR <75% implies immature to submature sediments, and ZTR >75% indicates mineralogical matured sediments. Apart from the ZTR index, various frequency percentage plot of both pie charts were made for each sample.

RESULTS AND DISCUSSION

Granulometric analysis

Eleven samples were used for the grain size analysis using standard sieve analysis techniques as outlined in [11].

Grain size statistical parameters. Table 1 shows the calculated values of various grain size parameters: the mean, median, skewness, kurtosis and standard deviation of the samples. The calculation of the multiple parameters follows [11].

Table 1 – Summary of the Interpretation of the Grain Size Statistical Parameters

Samples	Graphic Mean (Mz)	Graphic Standard Deviation (Sorting)	Graphic Skewness	Graphic Kurtosis
KA2	-0.47 / Very coarse sand	1.94 / Poorly sorted	0.12 / Fine skewed/ positively Skewed	0.94 / Mesokurtic
CHR	0.60 / Coarse sand	1.5 / Poorly sorted	0.15 / Fine skewed/ positively Skewed	0.94 / Mesokurtic
RYM1	-0.27 / Very coarse sand	1.8 / Poorly sorted	0.14 / Fine skewed/ positively Skewed	0.96 / Mesokurtic
GMS 1	-0.08 / Very coarse sand	1.75 / Poorly sorted	0.12 / Fine skewed/ positively Skewed	0.9 / Mesokurtic
RYM2	-0.53 / Very coarse sand	1.98 / Poorly sorted	0.08 / Nearly symmetrical	0.83 / Platykurtic
NGR	-0.13 / Very coarse sand	1.82 / Poorly sorted	0.08 / Nearly symmetrical	0.9 / Mesokurtic
GMS2	-0.13 / Very coarse sand	2.27 / Very Poorly sorted	0.15 / Fine skewed/ positively Skewed	0.86 / Platykurtic
BD2	0.20 / Coarse sand	1.29 / Poorly sorted	-0.01 / Nearly symmetrical	0.8 / Platykurtic
BD1	-0.27 / Very coarse sand	1.8 / Poorly sorted	0.12 / Fine skewed/ positively Skewed	0.91 / Mesokurtic
TNT	-0.40 / Very coarse sand	1.73 / Poorly sorted	0.12 / Fine skewed/ positively Skewed	0.87 / Platykurtic
DG1	-0.03 / Very coarse sand	1.71 / Poorly sorted	0.09 / Nearly symmetrical	0.94 / Mesokurtic

Table 2 – Result Showing Percentile Distribution of all Samples

Samples	KA2	CHR	RYM1	GMS 1	RYM2	NGR	GMS2	BD2	BD1	TNT	DG1
$\phi 5$	-3	-1.4	-2.7	-2.3	-3.1	-2.5	-3.1	-1.8	-2.6	-2.5	-2.2
$\phi 16$	-2.4	-0.9	-2.1	-1.85	-2.6	-2	-2.5	-1.2	-2.1	-2.2	-1.8
$\phi 25$	-1.8	-0.6	-1.6	-1.4	-2.1	-1.5	-1.9	-0.8	-1.6	-1.6	-1.2
$\phi 50$	-0.5	0.5	-0.4	-0.1	-0.5	-0.1	-0.3	0.2	-0.3	-0.4	0
$\phi 75$	1.0	1.5	0.8	1.2	1.0	1.2	1.4	1.2	1.0	1.0	1.2
$\phi 84$	1.5	2.2	1.7	1.7	1.5	1.7	2.4	1.6	1.6	1.4	1.7
$\phi 95$	3.4	3.4	2.9	3.4	3.2	3.4	3.8	2.1	3.2	3	3.3

Graphic mean (MZ). The graphic mean value for the samples ranges from -0.03 to 0.20 Φ (Table 1), i.e. from very coarse-grained to coarse-grained sandstones. The explicit mean values of all the samples indicate the predominance of very coarse-grained sandstone (10 samples), followed by coarse-grained sandstone (1 sample).

Graphic standard deviation (sorting). The values obtained from the samples range from 1.29 to 2.27 Φ (Table 1), indicating poorly sorted to very poorly sorted sandstones. The sorting degree indicates the hydrodynamic conditions (range of velocities and degree of turbidity) operating within the transporting medium. To some extent, it is suggestive of the travel distance [17].

Skewness. Skewness is a measure of the symmetry of the distribution, i.e. the proportion of coarse or fine fractions. It is instrumental in describing the depositional processes of the sediments. The skewness values derived from the samples range from -0.01 to 0.15 Φ, i.e., nearly symmetrical to finely skewed, respectively (Table 1). The values obtained are indicative of a fluvial environment.

Kurtosis. The kurtosis expresses the peakedness of the grain size distribution. The kurtosis values

of the samples range from 0.80 to 0.96 Φ, i.e. from platykurtic to mesokurtic, respectively (Table 1). The samples analyzed show a dominance of mesokurtic sediments (7 pieces). Although, little geologic information is derived from kurtosis values [24].

Probability plots. The probability plots are of environmental significance. They are indicative of either fluvial, beach, or wave zone, according to [26] characterization. Two sand populations indicate a fluvial setting, three sand populations indicate wave zone bars, and four sand populations show a beach setting. The probability curves were plotted from the data obtained from the sieve analysis. This is actually established from the plots of the cumulative weight percent against grain size in (phi, Φ).

From the Cumulative probability distribution curves of the analyzed samples, it is observed that all curves have only two sand population distributions (straight line segments).i.e. saltation and suspension. Thus, indicating a fluvial environment. [26, 7, 25].

Bivariate grain size parameters. Graphic Mean, Standard Deviation, Skewness and graphic First Percentile are the parameters used to separate sands based on origin according to standard plots devised by various workers. These bivariate plots include the field of mean versus the first percentile, standard deviation versus first percentiles, and standard deviation versus mean [13, 19]. Plots for each bivariate plot show that 100 % of the samples fall in the river sand environment.
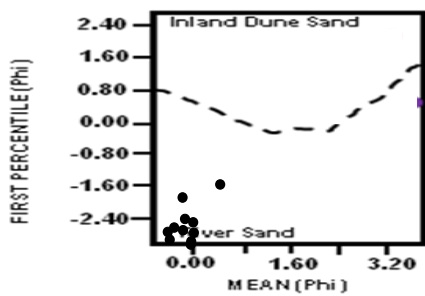

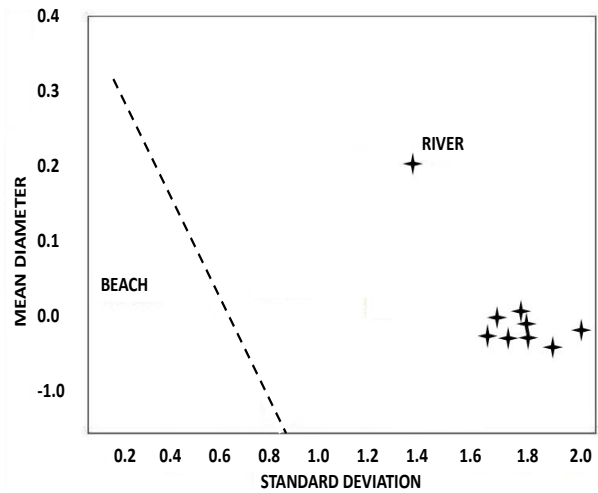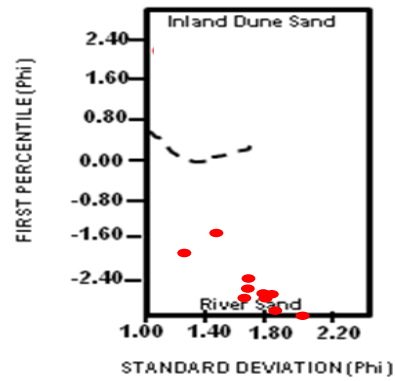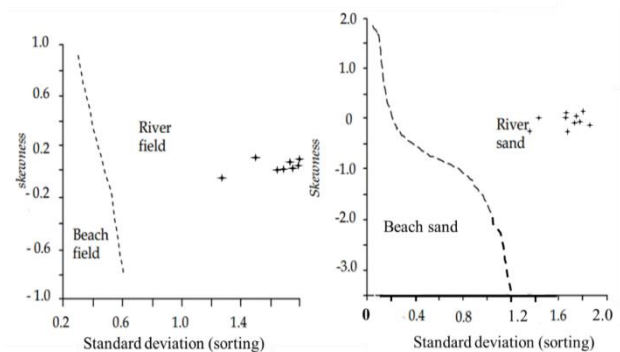Figure 2 − Bivariate plot of first percentile versus mean

Figure 3 and 4 − Bivariate plot of the first percentile against Standard Deviation and mean against standard deviation

Figures 5 − Bivariate plots of skewness against Standard Deviation

Petrography

Textural characteristics. Description of chosen thin sections of the stanniferous sandstone with focus on grain size, sorting, roundness, sphericity and grain contacts shows in Table 3.

Table 3 − Description of chosen thin sections of the stanniferous sandstone with a focus on grain size, sorting, roundness, sphericity and grain contacts

Samples	Grain size	Sorting	Roundness	Sphericity	Grain contact
KA2	Very coarse	Poorly sorted	Angular –sub angular	Low sphericity	Floating grains dominate, and no sutured contact
CHR	Very coarse	Poorly sorted	Angular –sub angular	Low sphericity	Floating grains dominate, and no sutured contact
RYM1	Very coarse	Poorly sorted	Angular –sub angular	Low sphericity	Floating grains dominate, and no sutured contact
GMS 1	Very coarse	Poorly sorted	Sub angular	Low sphericity	Floating grains dominate, with few point contacts and no sutured contact
NGR	Very coarse	Poorly sorted	Sub angular	Low sphericity	Floating grains dominate, with few point contacts and no sutured contact
GMS2	Coarse	Poorly sorted	Sub angular-poorly rounded	Low sphericity	Floating grains dominate, with few point contacts and no sutured contact
BD2	Very coarse	Poorly sorted	Angular –sub angular	Low sphericity	Floating grains dominate, and no sutured contact
BD1	Very coarse	Poorly sorted	Angular –sub angular	Low sphericity	Floating grains dominate, and no sutured contact
TNT	Very coarse	Poorly sorted	Angular –sub angular	Low sphericity	Floating grains dominate, with few point contacts and no sutured contact
DG1	Coarse	Poorly sorted	Angular –sub angular	Low sphericity	Floating grains dominate, with few point contacts and no sutured contact

Point counting. This involves identification and recording the amount of monocrystalline quartz (Qm), polycrystalline quartz (Qp), (Qm and Qp make together make the total quartz Qt), feldspar (F), lithic clasts L, opaque minerals (Op), cement and matrix. The result of the point count is given in Table 4.

Sandstone classification. The results from the point counting (Table 4) were used to determine the relative proportions of quartz, feldspar and lithic fragments in Table 5.

Table 4 − Results of point counting of the stanniferous sandstone thin section of the study area

Samples	Qm	Qp	Qt	F	L	Op	Cement / Matrix
KA2	249	0	249	0	0	9	42
CHR	255	7	262	0	0	7	31
RYM1	268	12	280	2	2	4	12
GMS 1	253	0	253	0	0	3	44
NGR	226	0	226	0	1	16	57
GMS2	245	0	245	0	2	12	41
BD2	276	9	285	0	0	2	13
BD1	271	0	271	4	0	13	12
DG1	286	0	286	3	0	4	7
TNT	269	0	269	0	0	12	19

Table 5 − Recalculated parameters through point counting used in various triangular plots for the provenance and sandstone classification of stanniferous sandstone of the study area

Samples	QFL (%)				QmFL (%)			
	Q	F	L	Total	Qm	F	L	Total
KA2	96.5	0.0	3.5	100	96.5	0.0	3.5	100
CHR	97.4	0.0	2.6	100	94.8	0.0	5.2	100
RYM1	97.2	0.7	2.1	100	93.1	0.7	6.3	100
GMS 1	98.8	0.0	1.2	100	98.8	0.0	1.2	100
NGR	93.0	0.0	7.0	100	93.0	0.0	7.0	100
GMS2	94.6	0.0	5.4	100	94.6	0.0	5.4	100
BD2	99.3	0.0	0.7	100	96.2	0.0	3.8	100
BD1	94.1	1.4	4.5	100	94.1	1.4	4.5	100
TNT	97.6	1.0	1.4	100	97.6	1.0	1.4	100
DG1	95.7	0.0	4.3	100	95.7	0.0	4.3	100

These were plotted on QFL and QmFLt diagrams to investigate provenance and highlight possible differences in sandstone composition (Figure 7). The design of the sandstones was classified in ternary QFL and QmFLt charts following the descriptive terms of [24] (Figure 7 A-B). Additionally, the same values were plotted on ternary QFL and QmFLt diagrams similar to [5] to highlight the samples' provenance (Figure 7 C-D). For the QFL diagram, all quartzose grains are plotted together, monocrystalline and polycrystalline quartz. Contrarily, the QmFLt diagram only re-

gards monocrystalline quartz as quartzose grains. Thus, in the QFL diagram used in this study, lithic clasts and opaque minerals are considered lithic fragments following [5]. For the QmFLt diagram, lithic fragments include polycrystalline quartz and opaque minerals, which agrees with the QmFLt chart [5] and is similar to the classification [20].

In the QFL and QmFLt diagrams, all the samples are classified as quartz arenites (Figure 7 A-B). After [5], the samples indicate a craton interior and recycled orogen source area (Figure 7 C-D).

Figure 8 – Photomicrographs of some selected samples in plane-polarized light (PPL) and cross-polarized light (CPL) showing poorly sorted and poorly rounded subangular grains (mag 100x)

Notes: Q = Quartz, OP = Opaque mineral

Heavy minerals. The ZTR Index calculated from the result of heavy minerals analysis for the selected samples varies from 35% to 78%, with an average index of 59%. The ZTR indices suggest that almost all the locations contain immature mineralogical sediments and have a short distance of travel except sample NGR which indicates mature mineralogical sediment.

Table 6 shows ilmenite is the highest identified mineral, ranging from 3 to 27 %. Cassiterite is the second most identified mineral, ranging from 2 to 14 %, followed by zircon (2 to 16 %), magnetite (0 to 17 %), tourmaline (5 to 11 %), rutile (2 to 8 %) and monazite (2 to 7 %). The lowest heavy mineral occurrence is garnet, with 0 to 5%.
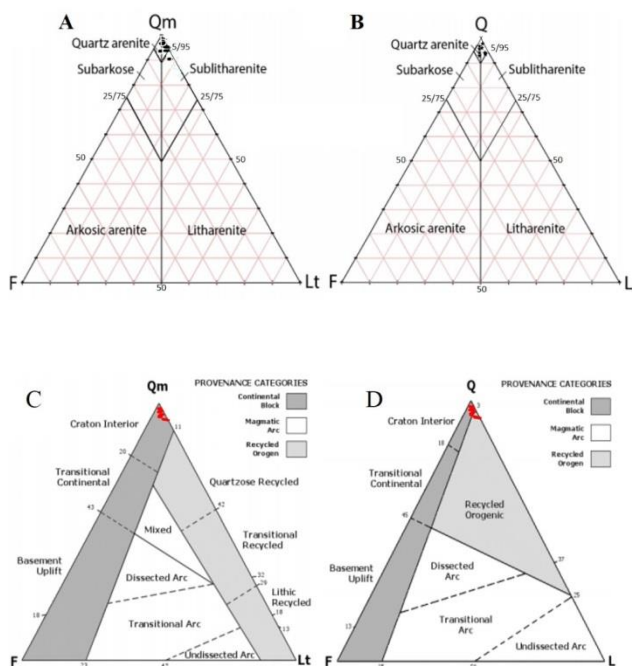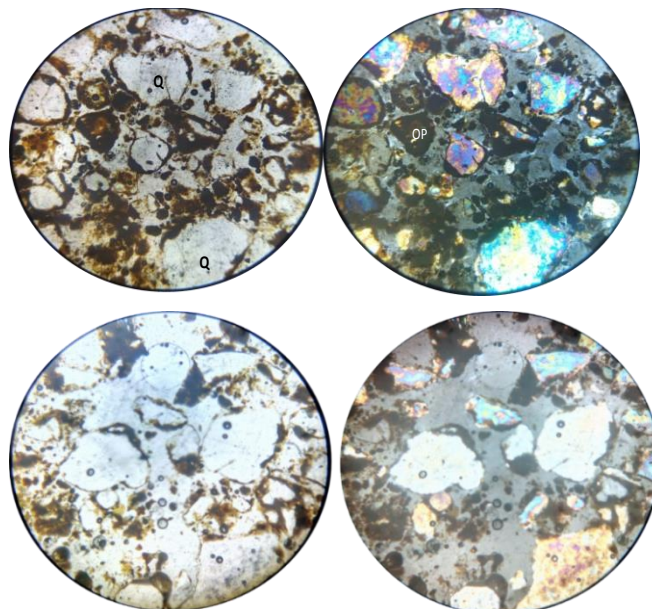
Figure 7 – QmFLt and QFL (A-D) diagrams showing the composition and classification, as well as the suggested provenance areas for the studied thin sections (A-B), modified from [24], while (C-D) are changed from [5]

Table 6 – Heavy minerals within the cassiterite bearing (stanniferous) sandstone in the study area

Samples	Zircon	Tourmaline	Rutile	Cassiterite	Monazite	Magnetite	Ilmenite	Garnet	Others	Total	ZTR	ZTR Index, %
BD1	18	23	15	19	12	7	13	8	94	209	56	59
BD2	22	17	12	22	14	3	22	7	85	204	51	54
KA2	4	13	7	27	9	13	28	9	93	203	24	35
CHR	24	13	16	20	7	20	28	2	78	208	53	65
TNT	15	15	8	23	5	43	47	2	90	248	38	56
DG1	23	12	12	5	15	13	36	4	107	227	47	66
RYM1	33	15	16	22	6	24	12	10	69	207	64	63
RYM2	26	15	5	18	12	15	33	0	79	203	46	61
NGR	32	18	8	4	9	0	59	2	86	218	58	79
GMS2	29	15	4	27	12	0	5	4	93	189	48	53
Total	226	156	103	187	101	138	283	48	874	2116	485	59
Average	22.6	15.6	10.3	18.7	10.1	13.8	28.3	4.8	87.4		48.5	59

Table 7 – Percentage composition of heavy minerals within the cassiterite bearing (stanniferous) sandstone in the study area, %

Samples	Zircon	Tourmaline	Rutile	Cassiterite	Monazite	Magnetite	Ilmenite	Garnet	Others	Total
BD1	9	11	7	9	6	3	6	4	45	100
BD2	11	8	6	11	7	1	11	3	42	100
KA2	2	6	3	13	4	6	14	4	46	100
CHR	12	6	8	10	3	10	13	1	38	100
TNT	6	6	3	9	2	17	19	1	36	100
DG1	10	5	5	2	7	6	16	2	47	100
RYM1	16	7	8	11	3	12	6	5	33	100
RYM2	13	7	2	9	6	7	16	0	39	100
NGR	15	8	4	2	4	0	27	1	39	100
GMS2	15	8	2	14	6	0	3	2	49	100
Total	11	7	5	9	5	7	13	2	41	100

The granulometric parameters have proved to be good indicators in distinguishing paleodepositional environments where fossils are lacking, especially in a continental setting.

The texture of sediments provides information about the medium, mode of transport, and energy conditions at the deposition time. The coarse to very coarse-grained nature of the sandstones encountered, bivariate analyses, univariate grain size parameters and probability plots, and the absence of fossils and trace fossils suggest deposition in a low-energy fluvial environment.

The petrological studies revealed that the stanniferous sandstones have similar mineralogical compositions and lithology types, although with few variations. The studies showed that quartz is the most dominant detrital mineral averaging about 93-99%. This is an indication that the sandstones are compositionally matured and texturally immature. It also implies a high degree of chemical weathering and closeness to the source. The quartz grains have grain sizes ranging from coarse to very coarse. They are poorly sorted, sub-angular to sub-rounded, with low sphericity. This also indicates a closeness to the source and textural immaturity. The grain contact is dominated by floating grains, with few point contacts and no sutured contact. Most grains show the presence of iron oxide rimming their edges, inclusions, and vacuoles, which could be attributed to a low-temperature source such as a hydrothermal vein. Quartz is the common silicate mineral acting as cement in the analytes, although there are a lot of patches of iron-oxide glue. These cementing materials are chemically attached to the crystal lattice of existing quartz grains forming rims of cement (overgrowths). The mineral content of cement is silica and iron-oxide. Feldspars were not observed in most thin sections, and the few presents have been significantly weathered, giving them a brown colouration. Very little feldspar suggests a slow sedimentation rate and a very high chemical weathering rate and indicates composition maturity.

The matrix is about 4 to 11% of the detrital fraction and consists of fine silty particles that appear brownish in some samples. This brownish colouration, coupled with the presence of iron oxide, is a strong indication of weathering and ferruginisation or probably due to percolation from the lateritic cover. Also, the reduction or oxidation process of the iron oxide may be responsible for this.

Judging from the ternary diagram, Both the QFL and QmFLt diagrams for sandstone classification indicates the dominance of quartz arenites, and following [5], the stanniferous sandstone samples are indicative of dominantly craton interior and few recycled orogen source area. Terrigenous sediments derived from the craton interior are more felsic, which explains why quartz minerals are more dominant.

From the study of the heavy mineral assemblages of the stanniferous sandstones of the studied area, it is found that zircon, tourmaline, rutile, cassiterite, ilmenite, magnetite, monazite and garnet occur persistently in all the studied samples. The heavy minerals were primarily derived from igneous and metamorphic rocks.

Opaque minerals (magnetite and ilmenite) indicate the chemical leaching of the sediments. Opaque minerals are mainly derived from crystalline igneous rocks, both acidic and basic. The higher proportion of opaque minerals indicates an igneous source. Therefore, the above study shows that the bulk of the heavies of the stannif-

erous sandstone are mineralogical immature and have been derived from igneous rocks and a little part from low to medium grade metamorphic rocks.

CONCLUSIONS

Stanniferous sandstones of the study area are dominantly angular to subrounded, coarse to very coarse-grained, poorly sorted, positively skewed, and mesokurtic sandstone. They were deposited in a fluvial environment by a low-energy fluvial (river) depositional system, and the deposition in proximal (close to the source). The heavy mineral study shows that the stanniferous sandstone is mineralogical immature and has been derived mainly from igneous rocks and a little part from low to medium-grade metamorphic rocks.

Furthermore, the stanniferous sandstones are compositionally matured, textural immature, close to the source and have experienced a high degree of chemical weathering.

REFERENCES

1. Basu, A. (2017). Evolution of Siliciclastic Provenance Inquiries. *Sediment Provenance*, 5–23. doi: 10.1016/b978-0-12-803386-9.00002-2

2. Batchelor, B. C. (1983). *Sundaland tin placer genesis and late Cenozoic coastal offshore stratigraphy in Western Malaysia and Indonesia* (Doctoral thesis), University of Malaya.

3. MacLeod, W. N., Turner, D. C., Wright, E. P., & Buchanan, M. S. (1971). *The geology of the Jos Plateau: explanation of 1:100 000 sheets nos. 147 148 168 169 and 189 and 190*. N. d.

4. Denyer, J. E. (1972). *The production of tin*. Paper no. 2: Conference on Tin Consumption, UK, London, International Tin Countries & Tin Resources Institute.

5. Dickinson, W., & Suczek, Ch. (1979). Plate Tectonics and Sandstone Compositions. *AAPG Bulletin, 63*. doi: 10.1306/2f9188fb-16ce-11d7-8645000102c1865d

6. Dickinson, W. R. (1985). Interpreting Provenance Relations from Detrital Modes of Sandstones. *Provenance of Arenites*, 333–361. doi: 10.1007/978-94-017-2809-6_15

7. Dike, E. F. (1972). *Sedimentology of the Lower Greensand of the Isle of Wight* (Doctoral thesis), University of Oxford.

8. Emery, K. O., & Noakes, L. C. (1968). Economic placer deposits of the continental shelf. *Technical Bulletin ECAFE, 1*, 95-111.

9. Fleet, W. F. (1926). Petrological Notes on the Old Red Sandstone of the West Midlands. *Geological Magazine, 63*(11), 505–516. doi: 10.1017/s0016756800085484

10. Folk, R. (1980). *Petrology of Sedimentary Rocks*. Austin: Hemphill Publication Company.

11. Folk, R. L., & Ward, W. C. (1957). Brazos River bar [Texas]; a study in the significance of grain size parameters. *Journal of Sedimentary Research, 27*(1), 3–26. doi: 10.1306/74d70646-2b21-11d7-8648000102c1865d

12. Folk, R. L. (1966). A review of grain-size parameters. *Sedimentology, 6*(2), 73–93. doi: 10.1111/j.1365-3091.1966.tb01572.x

13. Friedman, G. (1967). Dynamic Processes and Statistical Parameters Compared for Size Frequency Distribution of Beach and River Sands. *SEPM Journal of Sedimentary Research, 37*. doi: 10.1306/74d716cc-2b21-11d7-8648000102c1865d

14. Kankara, A. I., & Adagba, T. (2022). Geochemical investigation of gold and chalcophile minerals of Rawayau Area Katsina State, Nigeria. *Dutse Journal of Pure and Applied Sciences, 8*(2a), 126–139. doi: 10.4314/dujopas.v8i2a.14

15. Kinnaird, J. A., Nex, P. A. M., & Milani, L. (2016). Tin in Africa. *Episodes, 39*(2), 361–380. doi: 10.18814/epiiugs/2016/v39i2/95783

16. Kogbe, C. A. (Ed.). (1989). *Geology of Nigeria* (2nd ed.). Jos: Rock View International.

17. Krumbein, W. C., & Sloss, L. L. (1963). *Stratigraphy and Sedimentation* (2nd ed.). San Francisco: n. d.

18. Krumbein, W. C., & Pettijohn, F. J. (1938). *Manual of Sedimentary Petrography*. New York: D. Appleton-Century Crofts, Inc.

19. Moiola, R. J., & Weiser, D. (1968). Textural Parameters: an evaluation. *SEPM Journal of Sedimentary Research, 38*. doi: 10.1306/74d718c5-2b21-11d7-8648000102c1865d

20. Mørk, A., & Elvebakk, G. (1999). Lithological description of subcropping Lower and Middle Triassic rocks from the Svalis Dome, Barents Sea. *Polar Research, 18*(1), 83–104. doi: 10.3402/polar.v18i1.6559

21. Nagarajan, R., Armstrong-Altrin, J. S., Kessler, F. L., & Jong, J. (2017). Petrological and Geochemical Constraints on Provenance, Paleoweathering, and Tectonic Setting of Clastic Sediments From the Neogene Lambir and Sibuti Formations, Northwest Borneo. *Sediment Provenance*, 123–153. doi: 10.1016/b978-0-12-803386-9.00007-1

22. Ogunyele, A., & Akingboye, A. (2018). Tin Mineralisation in Nigeria: A Review. *Environmental and Earth Sciences Research Journal, 5*(1), 15–23. doi: 10.18280/eesrj.050103

23. Pettijohn, F. J. (1975). *Sedimentary Rock* (3rd ed.). New York: HarperCollins.

24. Pettijohn, F. J., Potter, P. E., & Siever, R. (1987). *Sand and Sandstone*. doi: 10.1007/978-1-4612-1066-5

25. Reineck, H.-E., & Singh, I. B. (1980). *Depositional Sedimentary Environments*. doi: 10.1007/978-3-642-81498-3

26. Visher, G. (1969). Grain Size Distributions and Depositional Processes. *SEPM Journal of Sedimentary Research, 39*. doi: 10.1306/74d71d9d-2b21-11d7-8648000102c1865d

27. Wright, J. B. (1970). Controls of mineralization in the older and younger tin fields of Nigeria. *Economic Geology, 65*(8), 945–951. doi: 10.2113/gsecongeo.65.8.945

28. Wright, J. B. (1985). The Younger Granites. *Geology and Mineral Resources of West Africa*, 129–137. doi: 10.1007/978-94-015-3932-6_15